Beyond Standard Echocardiography: Strain Imaging as the AI-Powered Key to Comprehensive Cardiac Function Evaluation

Samir Saha[1], Adnan Rahman[1], and Anatoli Kiotsekoglou[2]

[1]Region Stockholm
[2]Umea Universitet

April 05, 2024

Abstract

Strain imaging as a tool to engage in unravelling the secrets of cardiac motion in health and disease has opened a new horizon in the field of clinical cardiology beyond the standard algorithm for quantification of left ventricular function and dysfunction. As such, the wider application of strain can probably be compared with the ubiquitous application of the incretin molecule, glucagon like peptide 1 receptor agonist (GLP 1RA) first applied to manage type 2 diabetes, that is now indicated in many different conditions like obesity, heart failure, and Alzheimer's disease! This commentary would focus on the role of automated strain imaging in heart failure, aortic stenosis, cardiac amyloidosis, atrial fibrillation, left atrial, and right ventricular strain, on a 2-dimensional domain of spacetime navigated, to some extent, by AI. This commentary thus argues that automated strain imaging is becoming an essential tool for comprehensive cardiac assessment across various conditions.

Title page

Beyond Standard Echocardiography: Strain Imaging as the AI-Powered Key to Comprehensive Cardiac Function Evaluation

Authors:

Samir Saha [1] , Adnan Rahman[1] , and Anatoli Kiotsekoglou[2]

Affiliations:

[1] Acudoc cardiac imaging laboratory, Stockholm, and [2] Umeå University Hospital, Umeå, Sweden .

Address of Correspondence:

Samir K Saha. MD, PhD, FACC, FESC

Consultant Cardiologist,

Acudoc Cardiac Imaging Laboratory

Stockholm,

Sweden.

E mail: *samirksaha@gmail.com*

Phone: + 46 7351351756

X: @samirsaha

WhatsApp +46761001303

"Spacetime tells matter how to move; matter tells spacetime how to curve".

John Wheller, an American theoretical physicist explaining Einstein´s general theory of relativity.

Abstract :

Strain imaging as a tool to engage in unravelling the secrets of cardiac motion in health and disease has opened a new horizon in the field of clinical cardiology beyond the standard algorithm for quantification of left ventricular function and dysfunction. As such, the wider application of strain can probably be compared with the ubiquitous application of the incretin molecule, glucagon like peptide 1 receptor agonist (GLP 1RA) first applied to manage type 2 diabetes, that is now indicated in many different conditions like obesity, heart failure, and Alzheimer's disease! This commentary would focus on the role of automated strain imaging in heart failure, aortic stenosis, cardiac amyloidosis, atrial fibrillation, left atrial, and right ventricular strain, on a 2-dimensional domain of spacetime navigated, to some extent, by AI. This commentary thus argues that automated strain imaging is becoming an essential tool for comprehensive cardiac assessment across various conditions.

. . . .

Only about a few decades ago coronary artery disease (CAD) was the prime focus of cardiovascular research. Limitations in detection methods led to the exploration of new tools like tissue Doppler imaging (TDI). The European MYDISE data confirmed the potential of TDI in enhancing detection [1], as did those from Australia[2]. The investigators have shown that application of the velocity of left ventricular motion enhances the sensitivity and specificity of dobutamine stress echocardiography for detection of coronary artery disease, non-invasively.

In the review published in this issue of the journal by Gherbesia E et al [3] the authors have shown that the 2D speckle tracking strain imaging, built upon the foundation of TDI, is now a reliable tool for assessment and management of various cardiac conditions beyond CAD.

Atrial fibrillation: the story begins with the left atrium.

After half a dozen guidelines from the ACC, AHA, and ESC, the latest one for the first time ever recommends rhythm control as a first line management strategy either by ablation or by antiarrythmic drugs[4]. The document also elegantly presents criteria for selection of patients most suitable for ablation. Among others the size of the left atrium is the key. However, the size or the volume of the left atrium may not matter more than its mechanical integrity[5]. Kuppahally, et al [6] have shown the left atrial strain is a surrogate for fibrosis and the degree of fibrosis, and consequently magnitude of reservoir strain, depends on whether the AF is paroxysmal (less fibrosis, better strain) or persistent (more the fibrosis, worse is the strain). A just published paper has shown that an increased glucose (FDG-PET) metabolism in LA results in decreased LA strain: after successful ablation and restoration of sinus rhythm, the uptake of glucose decreases, and the longitudinal strain increases that coincides with decreased LA volume[7]. To negotiate the hydraulic and mechanical properties of the LA, the new AFI software provides biplane LA volume and all the three components of reservoir, conduit, and booster strain in no time (Figure 1). The AFI software in fact utilizes machine learning algorithms to automate LA volume and strain measurements, thereby significantly streamlining the process. We expect that in the not- too- distant future, cardiologists and electrophysiologists will utilize the ultra-modern SW for superfast assessment of LA size and strain at one go before considering ablation in eligible subjects.

Heart failure with preserved ejection fraction (HFPEF).

Although the currently available echo software does not use the large language model (LLM) based neural network characteristic of classic AI, the Mayo group [8] has used and LLM-AI algorithm to accurately diagnose HPPEF just by quantifying a single, apical 4- chamber cine-loop of the LV! Quite fascinating that the model not only could generate E/E´ ratio, but it also generated LV-GLS, on a 2-dimensional spacetime!

Aortic stenosis and myocardial work

It is known that severe aortic stenosis may lead to premature end of life, if untreated, as shown by the scholarly paper by Ross and Braunwald 54 years ago [9]. However, the question regarding timing of valve replacement is not a straightforward one for several reasons mainly subjective development of symptoms and objective evidence so called "collateral damage" (extra valvular damage due to sustained afterload increase). Serial follow up is therefore necessary to evaluate the progression of the disease. The 2020 ACC recommendations[10] has outlined a follow up interval for example in case of moderate disease. Keeping in mind that, it is also possible by analyzing myocardial work indices including global wasted work and global work efficiency to accurately predict valve area compared to traditional methods like the continuity equation, aiding in optimal decision-making for follow up prior to valve replacement (Figures, 2, 3).

The two familiar faces of thick hearts: hypertrophic cardiomyopathy (HCM) and cardiac amyloidosis (CA).

The two most recent triumphs of modern medicine have been the emergence of medical management of HCM and CA. In both the cases, therefore, accurate echocardiographic diagnosis is extremely important and strain imaging is mandatory, particularly for phenotyping differentiation of thick hearts. In HCM, all the three morphological distributions (sigmoid, reverse curve, apical) have distinct strain patterns, while in CA the demonstration of classic apical sparing of left ventricular longitudinal strain ("cherry on the top", one of the "red flags") always necessitates referral for further investigation to confirm CA (by hematologic, scintigraphic, genetic, histologic)[11].While apical strain is generally spared in CA, different regions within the apex may exhibit subtle variations in their response to pressure overload, as illustrated by differing pressure strain loops obtained by myocardial work. These variations highlight the regional differences in how these areas respond to demand of the poorly functioning heart (Figures 4,5). In case of hypertrophic cardiomyopathy, in which there clearly exists a gradient of strain within the Bull's eye plot differentiating HCM from CA, myocardial work indices may also uncover how a poorly functioning left ventricle distorting the pressure strain curve reminiscent of a stiff chamber despite preserved LVEF (Figure 6).

Right ventricle: The unforgettable chamber

For many years, the right ventricle received less attention than the left ventricle and was relegated to a Cinderella status. Human folly, as always have been, short lived, fortunately, and now we know that a modernist approach to improve quality of life (6-mimue walk test) and well-being of the RV (improved TAPSE) is at our disposal, as shown by the Triluminate trial [12]. Although the investigators have used TAPSE in the trial, it is possible to simultaneously compute TAPSE, RV strain and fractional area change (FAC%) at one go, using 2D strain in real time, providing a more comprehensive picture of RV systolic function. (Fig 7).

To conclude, the painstakingly written review [3]published simultaneously in this issue of the journal, the authors focused on the mechanistic, computational, and clinical aspects of speckle tracking strain imaging of the left ventricle. This document may stand out as a stand-alone reference guide for the application of strain in a wide variety of cardiac illnesses by novice and expert sonographers and cardiologists alike. Non only that, the review could be useful for the ultrasound physicists and engineers for future advancements in AI-powered strain imaging technologies, eventually contributing to improved diagnosis, prognosis, and management of various cardiac conditions. With that goal, it is time that we had an ultrafast, AI-driven full-proof tool for quantifying cardiac quadri-chamber mechanical function that can "revolutionize" cardiology[13] in a similar fashion as did Einstein´s $E= mc^2$ Given the superior spatial and temporal resolution of the modern stain software, this is no longer a distant dream, unlike in the cases of celestial bodies.

Figure Legends:

Legend to Fig 1

Simultaneous computation of biplane left atrial volume and strain (reservoir, conduit and booster strain) using the 2D strain software on images sampled at >60 Hz. Data obtained using the 3-click method (the 2 basal segments and at the roof of the atrium)

Legend to Fig 2

Application of indices of myocardial work in different phenotypes and grades of aortic stenosis (AS). Left panel: Low flow low gradient phenotype of severe AS with poor GWE, very low LV-GLS, and very high global wasted work, necessitating emergent referral for valve replacement. In comparison, a patient with moderate AS with preserved global work efficiency (GWE) (upper right) may have a delayed follow up while the patient in the lower right panel with reduced global wasted work (GWW), would require a follow up echo sooner than the one with preserved GWE.

Legend to Fig 3

Aortic valve area estimation using indices of myocardial work. Parameters included in the model are LVEF%, LV-GLS%, global work efficiency (GWE), global wasted work (GWW), global work index (GWI), and global constructive work (GCW). Significant p-values are in red.

Legend to Fig 4

Left ventricular longitudinal strain with apical sparing pattern in cardiac amyloidosis. The photo collage has been created just by 3- clicking the apical 3-chamber cine-loops. The AI based software searches the 2 other apical loops to compute the Bull´s eye with" cherry on the top" without any more human aid on the 2D spacetime with the LV in motion.

Legend to Fig 5

Myocardial work efficiency and the apical sparing strain: the differing pressure strain loops in different apical segments (the green pressure strain loops in panels B, C, and D) may suggest that the preserved apical strain may not be homogeneously distributed. Fig A is the global pressure strain loop in red. Bar diagrams: the green represents constructive work; blue represents wasted work. Pathophysiological significance of such heterogeneity is currently unknown.

Legend to Figures 6.

A patient with sigmoid type hypertrophic cardiomyopathy. On the right side a Bull´s eye plot, created by tracking 3 apical loops, shows regional strain gradients. On the left side myocardial work index showing a distorted and truncated pressure strain loop, suggesting a stiff left ventricle with low global strain and low work efficiency.

Legend to Fig 7

Fig 7. 2 D strain imaging of the right ventricle. Applying a "3-click" method that is by placing the cursor at the two basal and the third at the apical segment, the software simultaneously generates TAPSE, FAC% and global strain in no time, thereby facilitating an accurate assessment of RV systolic function.

Legend to the summary slide:

Application of left ventricular and left atrial strain to tell apart cardiac from non- cardiac dyspnea.

Upper left: a patient with non-cardiac dyspnea without elevation of filling pressure despite E/E´ratio 20. All other parameters are normal. Lower right: A patient with HFPEF and atrial fibrillation. Upper right. A patient with HFPEB in sinus rhythm showing significantly impaired LV-GLS% value. Lower right: Correlation between LA reservoir strain and NT-proBNP in a small cohort of HFPEF population in a primary care setting. The data emphasizes the value of incorporating LA strain in evaluating LV diastolic function/filling pressure [14].

Acknowledgements:

The authors would like to thank the Google´s Bard Chatbot for assisting us rephrasing some AI-related expressions used in this commentary. Part of the data in this commentary was presented at the quality

summit of the American College of Cardiology, October 2023 and at the Mayo Clinic´s Key Imaging Meeting, autumn 2023.

References

1. Mädler CF, Payne N, Wilkenshoff U, et al. Myocardial Doppler in Stress Echocardiography (MYDISE) Study Investigators. Non-invasive diagnosis of coronary artery disease by quantitative stress echocardiography: optimal diagnostic models using off-line tissue Doppler in the MYDISE study. Eur Heart J. 2003 Sep;24(17):1584-94. doi: 10.1016/s0195-668x(03)00099-x. PMID: 12927194.
2. Cain P, Baglin T, Case C, Spicer D, Short L, Marwick TH. Application of tissue Doppler to interpretation of dobutamine echocardiography and comparison with quantitative coronary angiography. Am J Cardiol. 2001 Mar 1;87(5):525-31. doi: 10.1016/s0002-9149(00)01425-9. PMID: 11230833
3. Gherbesia E, Silvia Gianstefani S, Angelib F, et al. Myocardial strain of the left ventricle by speckle tracking echocardiography: from physics to clinical practice. Echocardiography 2024:XX;XX
4. Wiggins BS, Cibotti-Sun M, Moore MM. 2023 Atrial Fibrillation Guideline-at-a-Glance. J Am Coll Cardiol. 2024 Jan 2;83(1):280-284. doi: 10.1016/j.jacc.2023.10.021. Epub 2023 Nov 30. PMID: 38043044.
5. Saha SK, Andersson PL. Giuseppe C, et al. Global left atrial strain Correlates with $CHADS_2$ risk Score in patients with atrial fibrillation.J AmM Soc Echocardiogr 2011 Volume 24, Issue 5, 506 – 512
6. Kuppahally SS, Akoum N, Burgon NS, Badger TJ, Kholmovski EG, Vijayakumar S, et al. Left atrial strain and strain rate in patients with paroxysmal and persistent atrial fibrillation: relationship to left atrial structural remodeling detected by delayed-enhancement MRI. Circ Cardiovasc Imaging. 2010;3(3):231–9.
7. Marchandise, S, Roelants, V, Raoult, T. et al. Left Atrial Glucose Metabolism Evaluation by ^{18}F-FDG-PET in Persistent Atrial Fibrillation and in Sinus Rhythm. *J Am Coll Cardiol Basic Trans Science.* null2024, 0 (0) *.https://doi.org/10.1016/j.jacbts.2023.11.001*
8. Akerman AP, Porumb M, Scott CG, Beqiri A, Chartsias A, Ryu AJ, et al. Automated echocardiographic detection of heart failure with preserved ejection fraction using artificial intelligence. JACC Adv. 2023;2(6):100452.
9. Ross J Jr, Braunwald E. Aortic stenosis. Circulation. 1968;37/38(suppl V): V-61–V-67
10. Otto CM, Nishimura RA, Bonow RO, et al. 2020 ACC/AHA Guideline for the management of patients with valvular heart disease: Executive Summary: A Report of the American College of Cardiology/American Heart Association Joint Committee on Clinical Practice Guidelines. Circulation. 2021 Feb 2;143(5):e35-e71.
11. Garcia-Pavia P, Rapezzi C, Adler Y, et al. Diagnosis and treatment of cardiac amyloidosis: a position statement of the ESC Working Group on Myocardial and Pericardial Diseases. Eur Heart J. 2021 Apr 21;42(16):1554-1568. doi: 10.1093/eurheartj/ehab072. PMID: 33825853; PMCID: PMC8060056.
12. von Bardeleben RS, Lurz P, Sorajja P, et al. Two-year outcomes for tricuspid pepair with a transcatheter Edge-to-Edge Valve Repair From the Transatlantic TRILUMINATE Trial. Circ Cardiovasc Interv. 2023 Aug;16(8):e012888.
13. Machteld JB, Davy W, Jason HM, Graciela G-H, Folkert WA, Artificial intelligence: revolutionizing cardiology with large language models, *European Heart Journal* , 2024;, ehad838, https://doi.org/10.1093/eurheartj/ehad838
14. Smiseth OA, Morris DA, Cardim N, et al. Multimodality imaging in patients with heart failure and preserved ejection fraction: an expert consensus document of the European Association of Cardiovascular Imaging. Eur Heart J Cardiovasc Imaging. 2022 Jan 24;23(2):e34-e61. doi: 10.1093/ehjci/jeab154. PMID: 34729586.

Fig 1. Simultaneous computation of biplane left atrial volume and strain (reservoir, conduit and booster strain) using the 2D strain software on images sampled at >60 Hz. Data obtained using the 3-click method (the 2 basal segments and at the roof of the atrium)

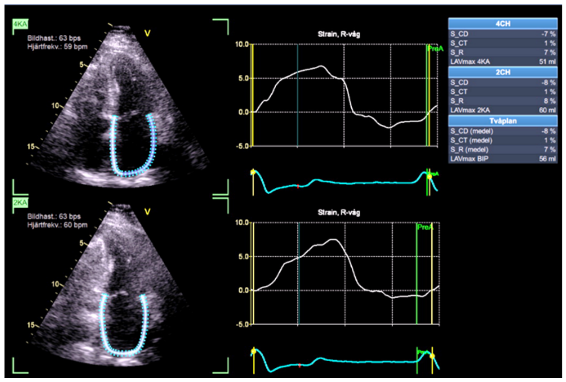

Fig 2. Application of indices of myocardial work in different phenotypes and grades of aortic stenosis

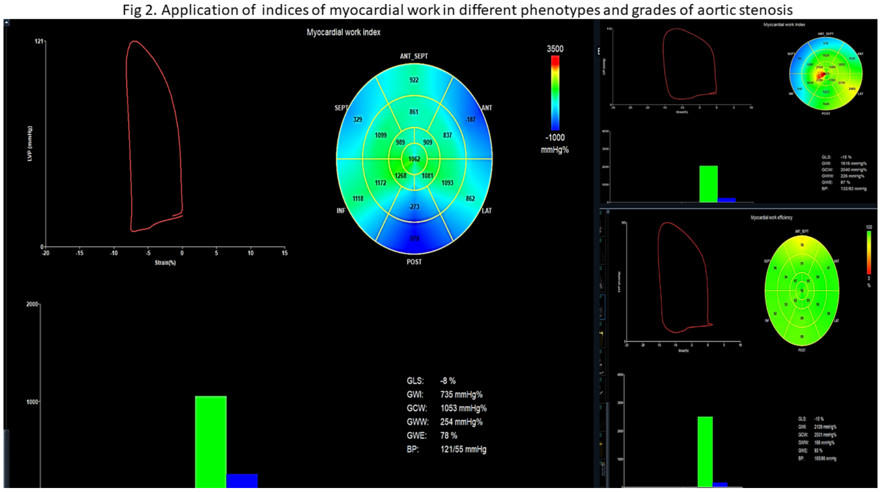

Fig 3 : Aortic valve area estimation using indices of myocardial work. Parameters included in the model are LVEF%, LV-GLS%, global work efficiency (GWE), global wasted work (GWW), global work index (GWI), and global constructive work (GCW). Significant p-values are in red.

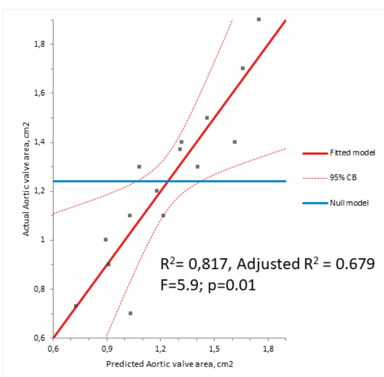

Parameter	Estimate	95% CI	SE	t	p-value
Constant	14,67	5,784 to 23,55	3,8525	3,81	0,0052
LVEF	0,04659	0,01032 to 0,08286	0,015729	2,96	0,0181
LV-GLS%	0,01803	-0,06963 to 0,1057	0,038015	0,47	0,6480
Global Work Efficiency %	-0,1752	-0,2707 to -0,07965	0,041417	-4,23	0,0029
GWW, mmHg%	-0,009648	-0,01511 to -0,004185	2,3690E-03	-4,07	0,0036
GWI, mmHg%	-0,001111	-0,002351 to 1,303E-04	5,3808E-04	-2,06	0,0729
GCW, mmHg%	0,001732	4,698E-04 to 0,002994	5,4737E-04	3,16	0,0133

Fig 4. Left ventricular longitudinal strain with apical sparing pattern in cardiac amyloidosis. The photo collage has been created just by 3-clicking the apical 3-chamber cine-loops. The AI based software searches the 2 other apical loops to compute the Bull´s eye with" cherry on the top" without any more human aid on the 2D spacetime with the LV in motion.

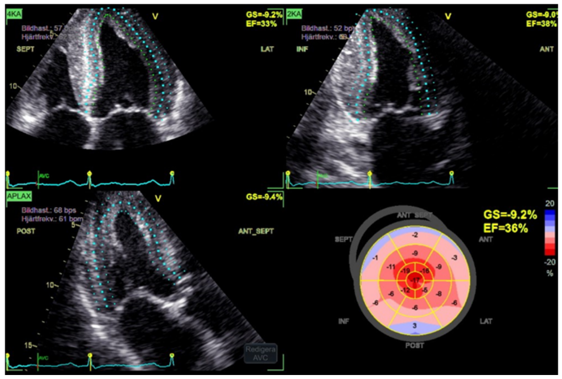

Fig 5. Myocardial work efficiency and the apical sparing strain: the differing pressure strain loops in different apical segments (the green pressure strain loops in panels C, and D) may suggest that the preserved apical strain may not be homogeneously distributed. Fig A is the global pressure strain loop in red. Bar diagrams: the gre represents constructive work; blue represents wasted work. Pathophysiological significance of such heterogeneity is currently unknown.

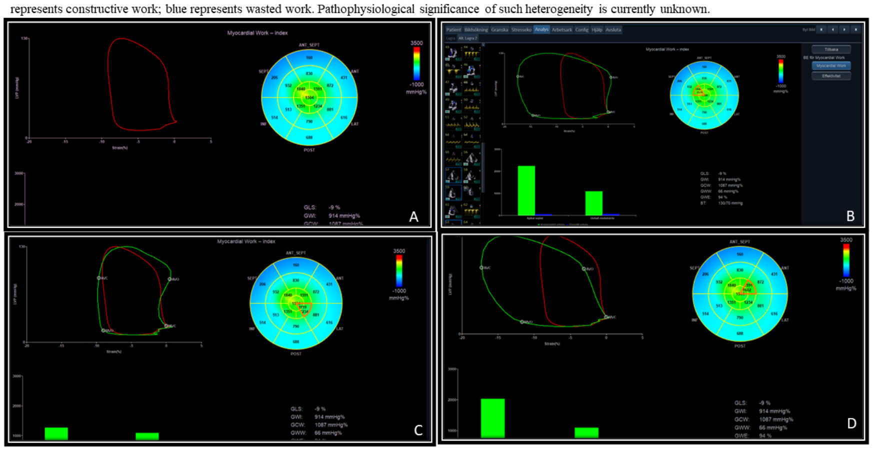

Figure 6. A patient with sigmoid type hypertrophic cardiomyopathy. On the right side a Bull´s eye plot, created by tracking 3 apical loops, shows regional strain gradients. On the left side myocardial work index showing a distorted and truncated pressure strain loop, suggesting a stiff left ventricle with low global strain and low work efficiency.

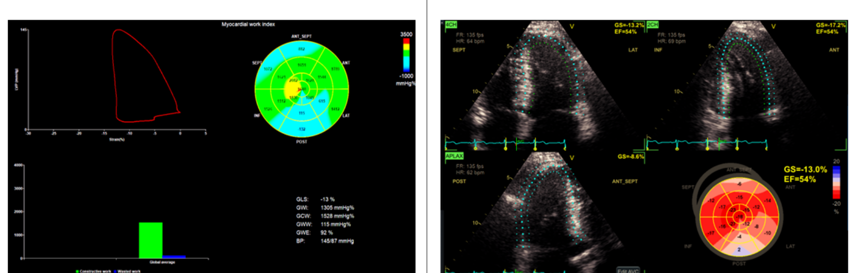

Fig 7. 2D strain imaging of the right ventricle. Applying a ”3-click” method that is by placing the cursor at the two basal and the third at the apical segment, the software simultaneously generates TAPSE, FAC% and global strain in no time, thereby facilitating an accurate assessment of RV systolic function.

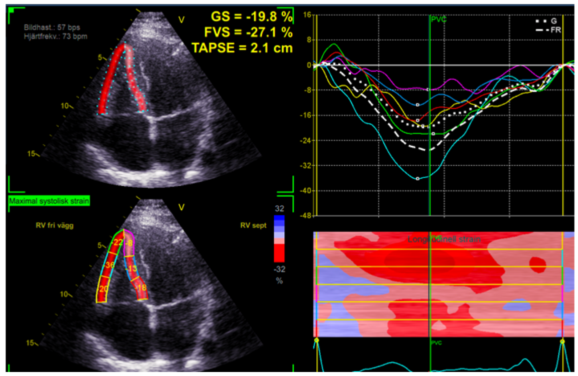

Graphic abstract

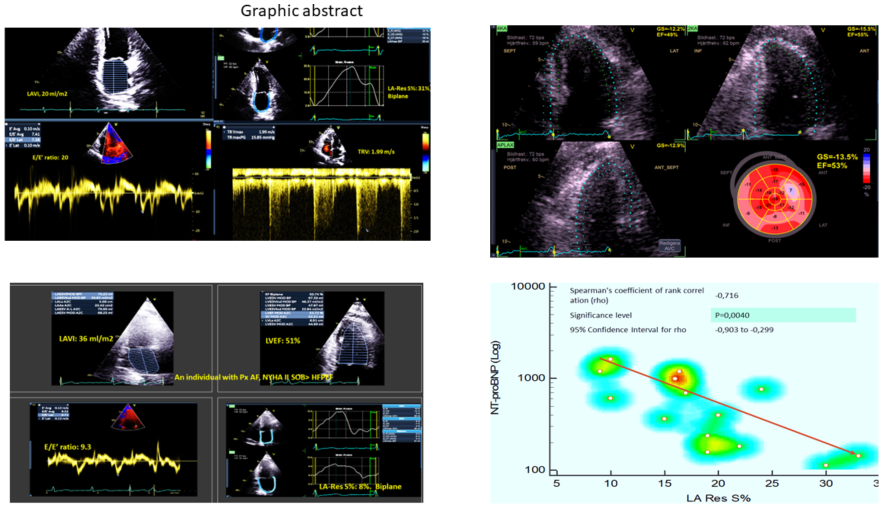

Fig 1. Simultaneous computation of biplane left atrial volume and strain (reservoir, conduit and booster strain) using the 2D strain software on images sampled at >60 Hz. Data obtained using the 3-click method (the 2 basal segments and at the roof of the atrium)

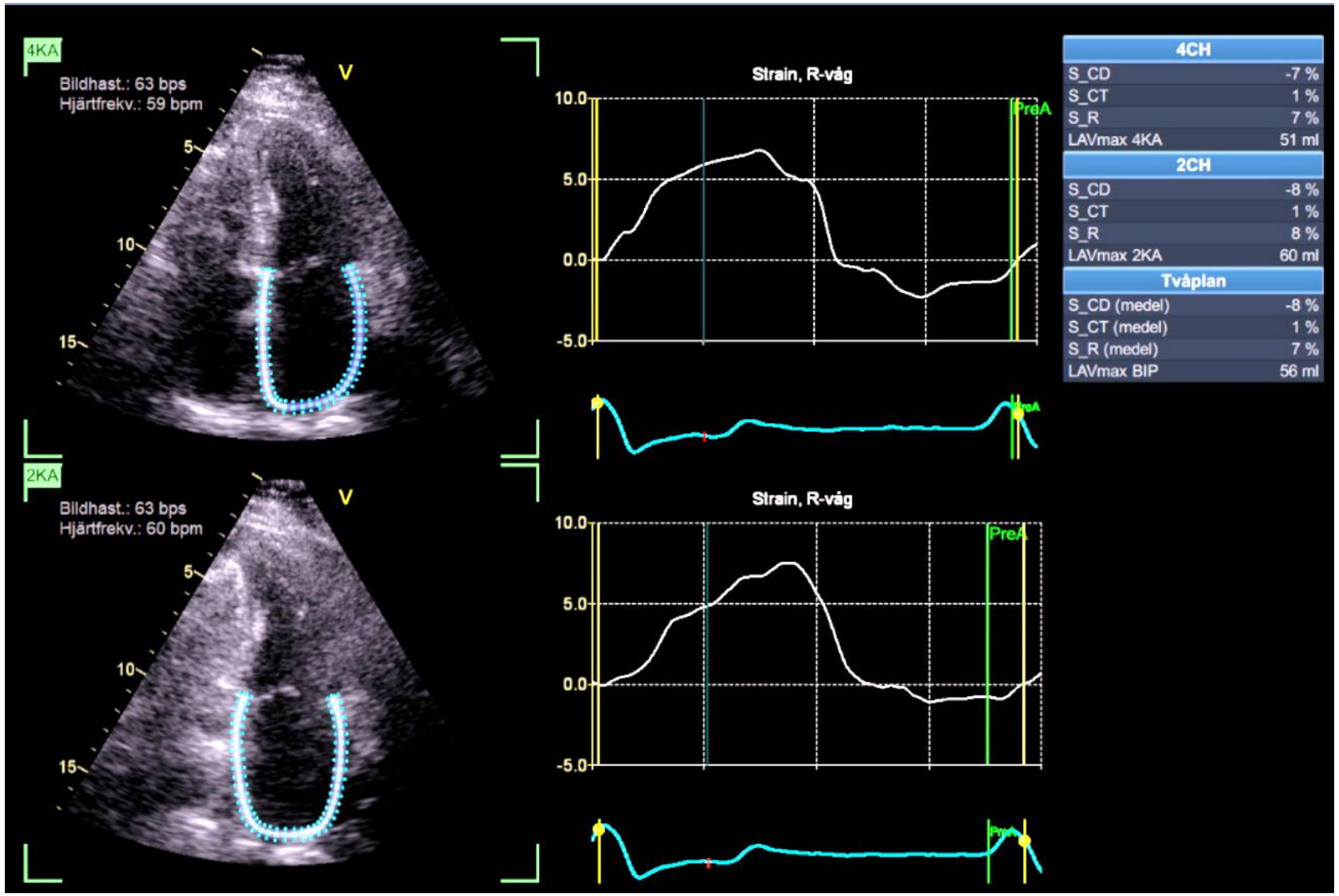

Fig 2. Application of indices of myocardial work in different phenotypes and grades of aortic stenosis

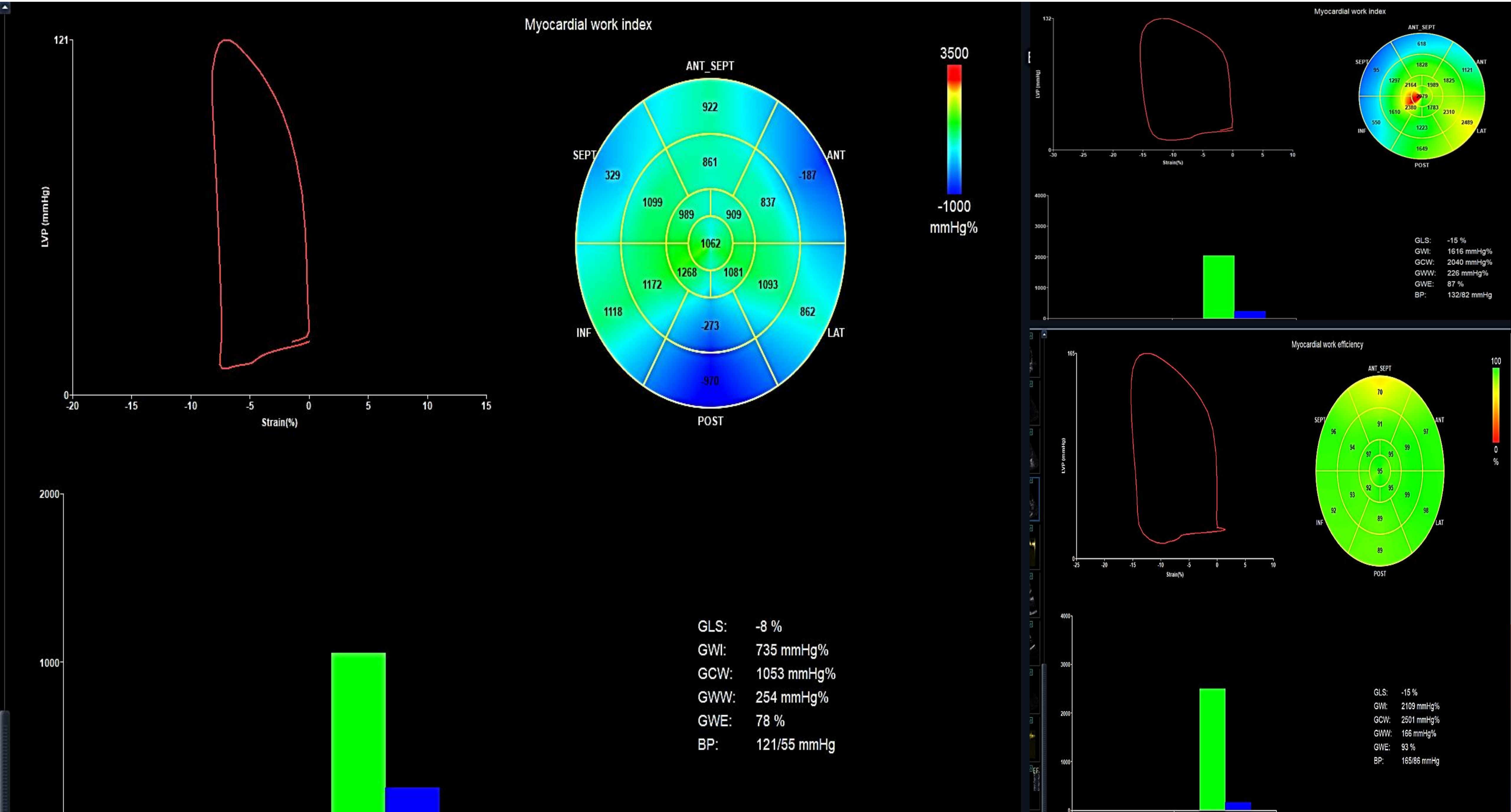

Fig 3 : Aortic valve area estimation using indices of myocardial work. Parameters included in the model are LVEF%, LV-GLS%, global work efficiency (GWE), global wasted work (GWW), global work index (GWI), and global constructive work (GCW). Significant p-values are in red.

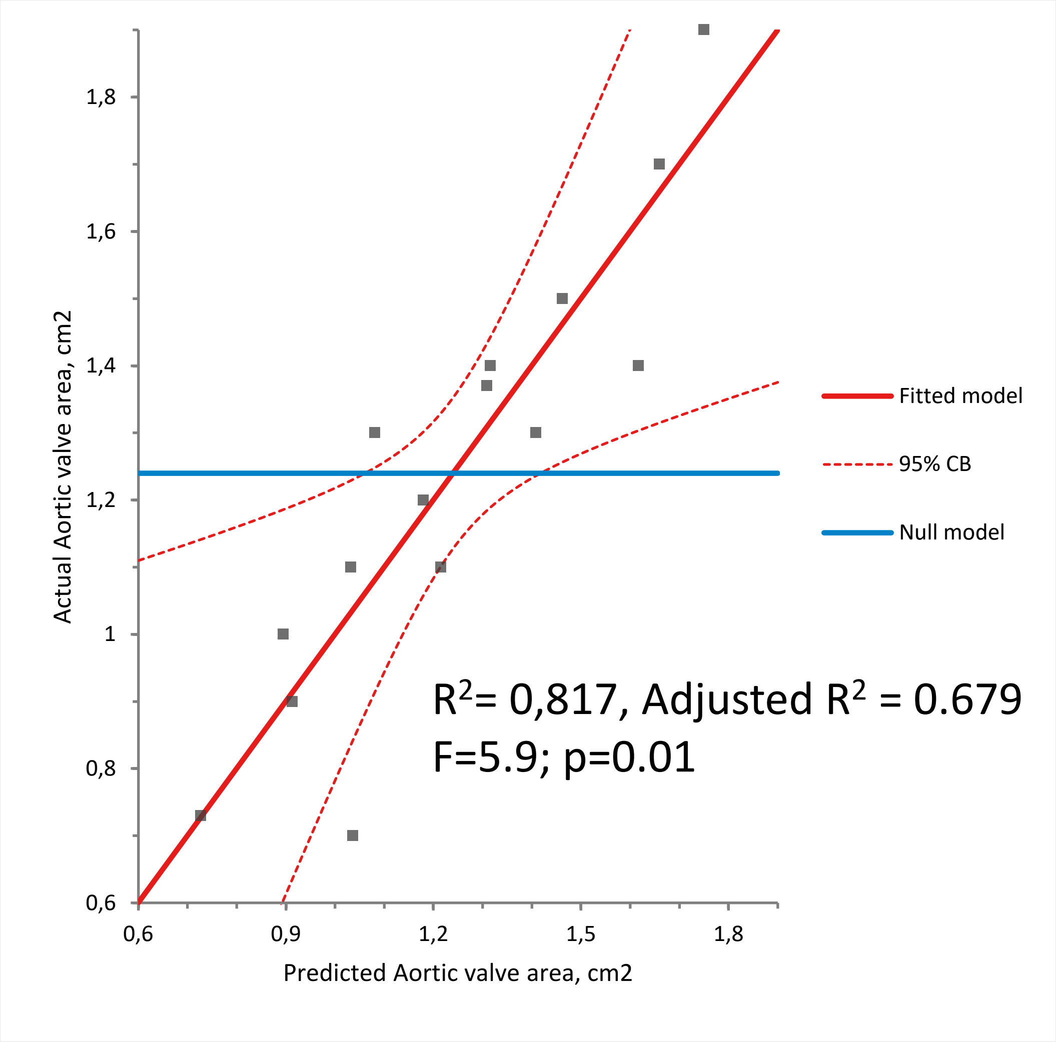

Parameter	Estimate	95% CI	SE	t	p-value
Constant	14,67	5,784 to 23,55	3,8525	3,81	0,0052
LVEF	0,04659	0,01032 to 0,08286	0,015729	2,96	0,0181
LV-GLS%	0,01803	-0,06963 to 0,1057	0,038015	0,47	0,6480
Global Work Efficiency %	-0,1752	-0,2707 to -0,07965	0,041417	-4,23	0,0029
GWW, mmHg%	-0,009648	-0,01511 to -0,004185	2,3690E-03	-4,07	0,0036
GWI, mmHg%	-0,001111	-0,002351 to 1,303E-04	5,3808E-04	-2,06	0,0729
GCW, mmHg%	0,001732	4,698E-04 to 0,002994	5,4737E-04	3,16	0,0133

Fig 4. Left ventricular longitudinal strain with apical sparing pattern in cardiac amyloidosis. The photo collage has been created just by 3-clicking the apical 3-chamber cine-loops. The AI based software searches the 2 other apical loops to compute the Bull´s eye with" cherry on the top" without any more human aid on the 2D spacetime with the LV in motion.

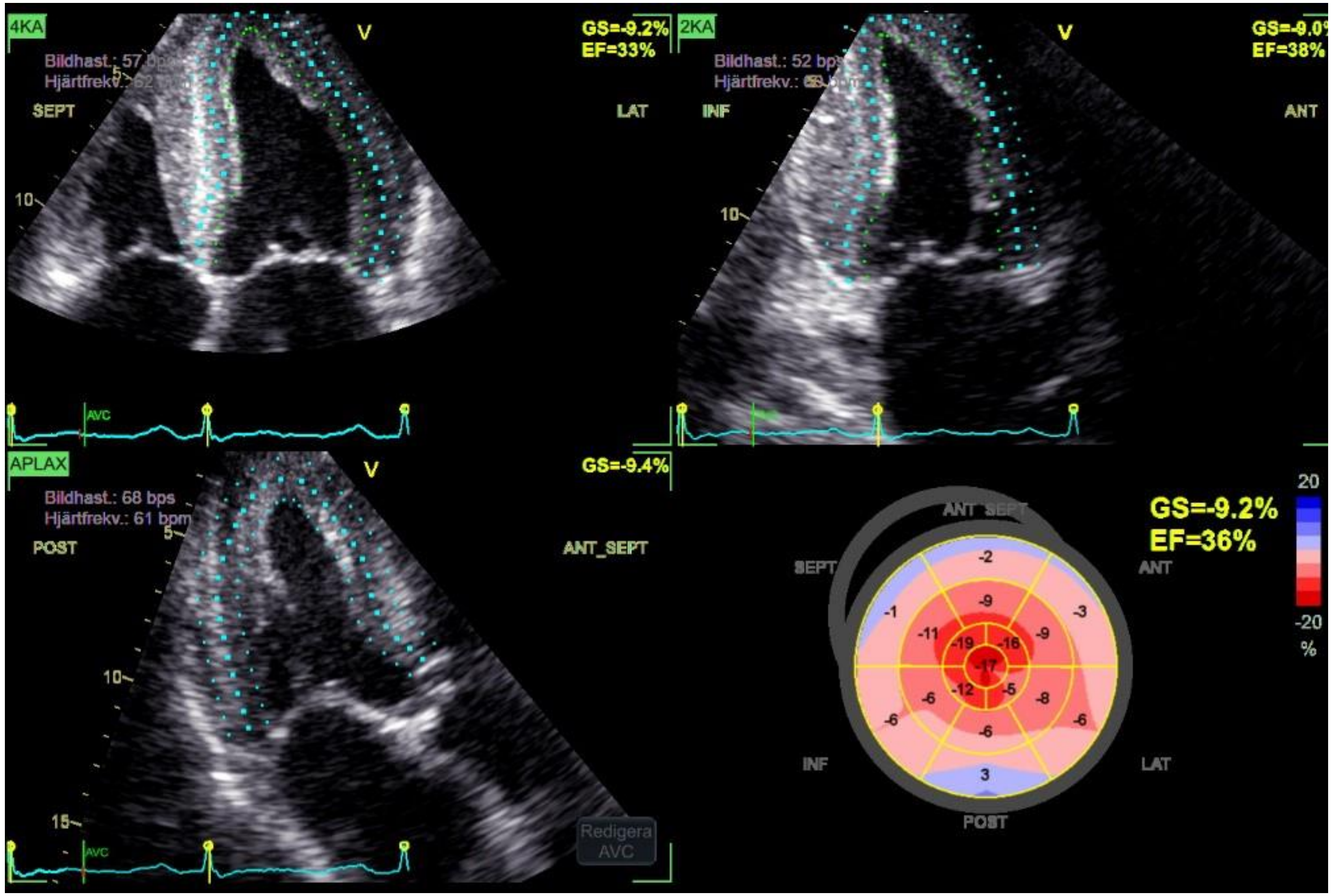

Fig 5. Myocardial work efficiency and the apical sparing strain: the differing pressure strain loops in different apical segments (the green pressure strain loops in panels C, and D) may suggest that the preserved apical strain may not be homogeneously distributed. Fig A is the global pressure strain loop in red. Bar diagrams: the gre represents constructive work; blue represents wasted work. Pathophysiological significance of such heterogeneity is currently unknown.

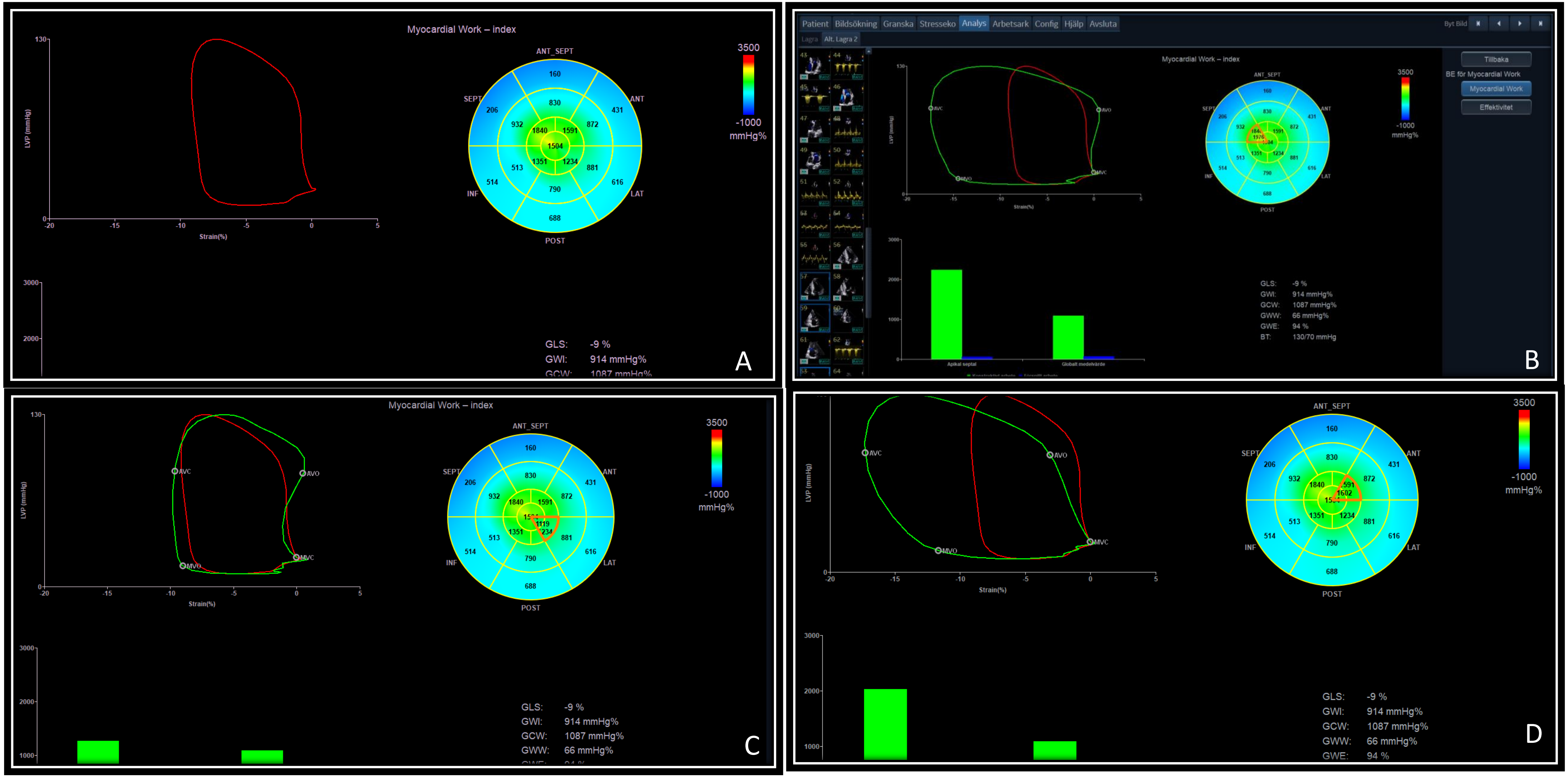

Figure 6. A patient with sigmoid type hypertrophic cardiomyopathy. On the right side a Bull´s eye plot, created by tracking 3 apical loops, shows regional strain gradients. On the left side myocardial work index showing a distorted and truncated pressure strain loop, suggesting a stiff left ventricle with low global strain and low work efficiency.

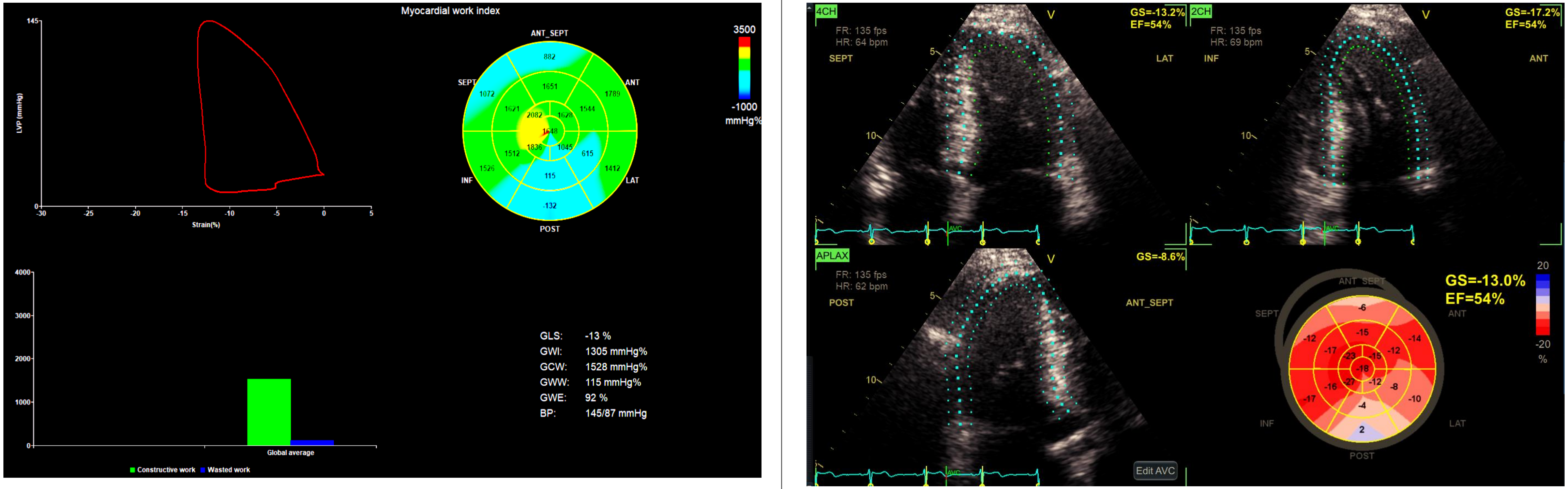

Fig 7. 2D strain imaging of the right ventricle. Applying a ”3-click” method that is by placing the cursor at the two basal and the third at the apical segment, the software simultaneously generates TAPSE, FAC% and global strain in no time, thereby facilitating an accurate assessment of RV systolic function.

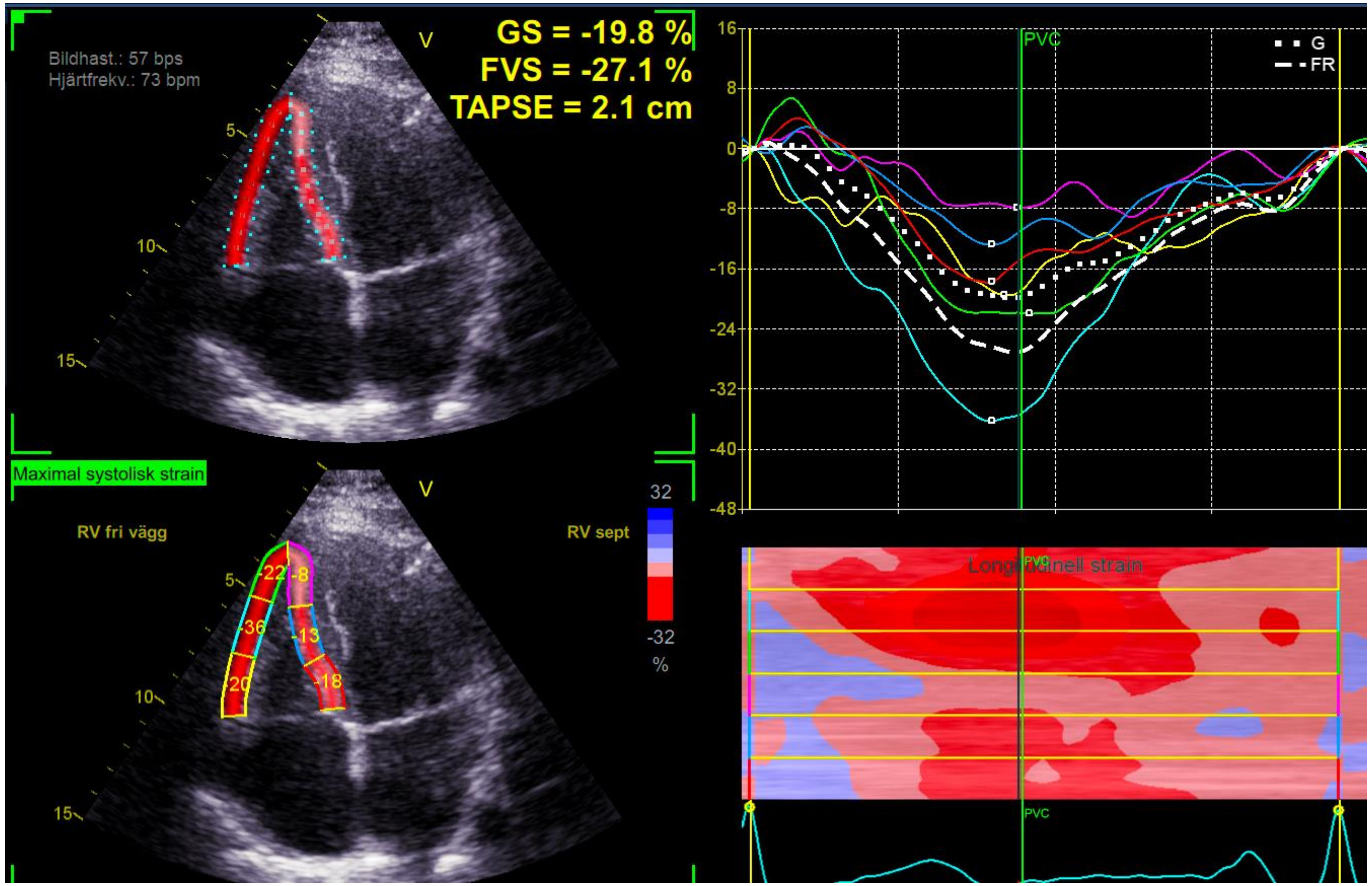

Graphic abstract